

A CPD Image Sensor with P-well Antiblooming Structure

Kohji SENDA, Sumio TERAOKA, Yoshimitsu HIROSHIMA,
Yuji MATSUDA, Shigenori MATSUMOTO and Takao KUNII

Semiconductor Laboratory, Matsushita Electronics Corporation

Takatsuki, Osaka 569, Japan

A CPD image sensor with an anti-blooming function by a p-well instead of the conventional overflow drain structure, is proposed. The potential profile along the depth in the p-well has been simulated by applying the linearly graded junction approximation to the numerical integration of the Poisson equation. Based on the simulation results, a new CPD image sensor with the anti-blooming p-well structure has been designed and fabricated. It has been proved that the p-well CPD organization is strikingly effective to the blooming suppression. In addition, the horizontal resolution has been increased by the application of the checker-pattern arrangement of photodiodes in the image area, from which the overflow drains had been removed.

§1. Introduction

In recent years, solid-state image sensors with CCD or MOS configuration have rapidly progressed for the application to single-chip color video cameras.^{1) 2)} The authors have proposed a unique CPD (Charge Priming Device) image sensor, in which X-Y arrayed photodiodes with MOS switches are combined with analog CCD readout shift registers through charge priming transfer (CPT) couplers.³⁾ The CPD sensor has inherent advantages such as low noise, wide dynamic range and no fixed-pattern noise. For suppression of the blooming phenomenon due to over-exposure, the overflow drain structure has been used so far. The organization, however, inevitably reduces the photo-sensitive area, making the pattern of the image area complicated.

This paper describes a new organization of the CPD image sensor, in which a p-well structure, instead of the overflow drain structure, is utilized for the blooming suppression. Among four constituent p-well islands in the sensor, the p-well for the image area has been designed much shallower than the other p-wells so as to be completely depleted during operation. In order to clarify the blooming suppression effect of the p-well structure, the potential profile along the depth in the p-well has been simulated by applying the linearly graded junction approximation to the numerical integration of the Poisson equation.

§2. Design Considerations

2.1 Device structure

The block diagram and the schematic cross-sectional view of the CPD image sensor with the p-well structure are shown in Fig. 1 and Fig. 2, respectively. On an N-substrate, are formed four p-well islands: PW1 for the image area of arrayed photodiodes with MOS switches, PW2 for the CPT couplers and the CCD readout shift registers, PW3 for the vertical MOS shift registers and PW4 for the protection diodes against negative pulse voltage. These p-wells are reversely biased with respect to the N-substrate during operation. One of the most important advantages of this p-well organization is that the impurity profile in PW1 can be selected independently of those in the other p-wells. If the potential profile in PW1 along the

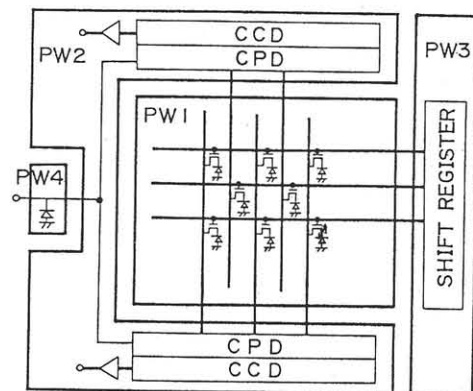


Fig. 1 Block diagram of the CPD with p-well structure.

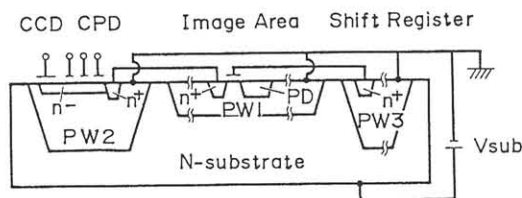


Fig. 2 Schematic cross-sectional view of CPD with p-well structure.

depth is appropriate, excess electrons generated by over-exposure may flow into the N-substrate, ensuring blooming suppression.

2.2 Simulation of potential profile

The potential profiles in the p-well for the image area have been simulated along the following procedure. The impurity distributions across the p-well/N-substrate junction and the n^+ /p-well junction have been approximated by two linearly graded junctions as shown in Fig. 3 (a). The field distributions F1, F2, F3, and F4 in Fig. 3 (b) were obtained through the numerical integration of the one-dimensional Poisson equation for four sets of the space charge regions. The field profile F1 corresponds to the extremity case in which the N-substrate is no longer depleted. Integration of the fields gives the respective potentials as shown in Fig. 3 (c), where the N-substrate is assumed to be biased by $V_{sub} = 10$ V in respect to the p-well.

In the figure, the extremity field profile F1 in Fig. 3 (b) results in the potential profile P1, along which electrons start to be injected from the N-substrate to the n^+ -region. Consequently, the potential in the n^+ -region cannot be reset lower than that of P1, where the potential difference between the n^+ -region and N-substrate is defined as the injection potential ϕ_{inj} . With increasing the number of electrons stored in the photodiode, the number of ionized donors in the n^+ -region decreases, while in the N-substrate it increases to maintain the neutrality condition. As a result, the potential in the n^+ -region shifts upwards to P4 from P1, P2 and P3 in Fig. 3 (c). Finally the potential profile P4 is reached, where the space charge region in the n^+ -region completely disappears as illustrated by the field distribution F4 in Fig. 3 (b). Under this condition, the excess electrons generated in the photodiode by over-exposure can flow towards the N-substrate,

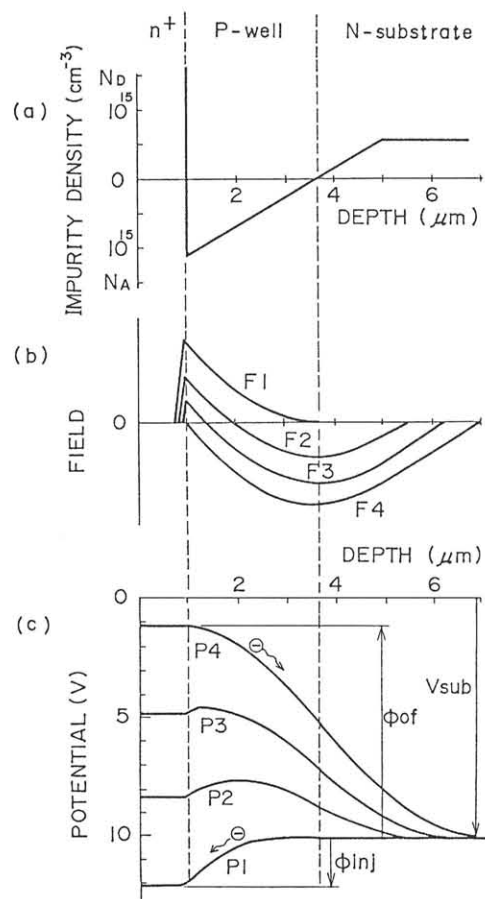


Fig. 3 The photodiodes in Pw1. (a) impurity density vs. depth. (b) field distribution. (c) potential variation vs. depth.

whose potential is lower by the overflow potential ϕ_{of} . This is the criterion for the anti-blooming condition that excess electrons can not spill out laterally to the neighboring photodiodes. For the blooming suppression the voltage applied to the N-substrate V_{sub} must be sufficiently higher than the overflow potential ϕ_{of} , which is determined by the impurity distribution around the P-well/N-substrate junction. The dynamic range of a photodiode may be expressed in terms of $(V_R + \phi_{of} - V_{sub})$, where V_R is the reset voltage for the photodiode and is always lower than $(V_{sub} + \phi_{inj})$ as previously mentioned.

§3. Experiments

3.1 P-well characteristics

The new CPD image sensors with the p-well structure were fabricated on about $10\Omega\text{cm}$ N-type silicon substrate by the n-channel poly-silicon gate technology. The impurity profiles in the p-wells were controlled with the dose of implanted B^+ -ions and the annealing condition. The new

device has particularly been designed for use in the PAL system, where 398(H) x 588(V) photodiodes are arranged in a checker pattern on the image area of 8.8 mm(H) x 6.6 mm(V) (See Fig. 1).

3.2 Potential profile in the p-well

Figure 4 shows the spreading resistance profile measured in the p-well for the image area. The curve shows the junction depth to be 3.5 μm . It is also verified that the linearly graded junction approximation, which has been assumed upon the potential profile calculation in section 2.2, is quite reasonable.

The overflow potential ϕ_{of} and the injection potential ϕ_{inj} were measured by using a curve tracer inserted between the n^+ -region and the N-substrate biased against the p-well. The measured potentials, ϕ_{of} and ϕ_{inj} , are plotted in Fig. 5 as functions of the dose of B^+ implantation into the N-substrate for p-well formation. In the figure are also shown with the solid curves the potentials calculated using the junction depth obtained from the spreading resistance. The agreement with the experimental results are excellent. It is seen that the magnitude of the overflow potential ϕ_{of} pronouncedly increases with the increase in the dose of implanted B^+ . This in turn indicates that at a high implantation dose a high voltage is required for V_{sub} to suppress blooming, which may be practically limited up to around 15 V in the operating circuit. On the other hand, the low dose implantation will narrow the dynamic range of photodiodes which is given in term of $(V_R + \phi_{of} - V_{sub})$ as discussed in section 2.2. In view of these results the dose of B^+ implantation for formation of the image area p-well has been determined to be $5-6 \times 10^{11}$ ions/cm².

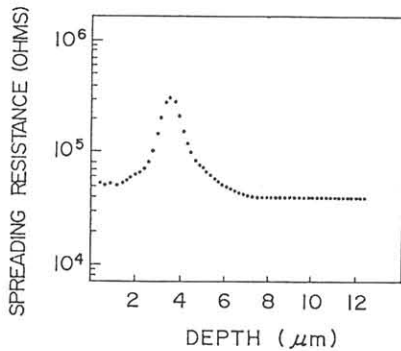


Fig. 4 The spreading resistance profiles measured in the p-well for the image area.

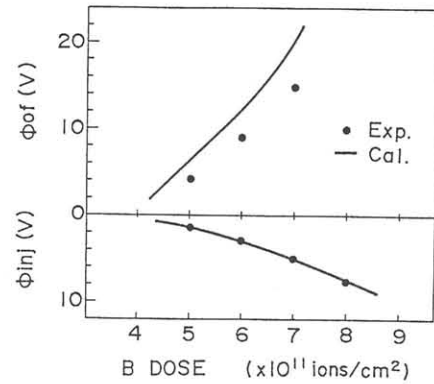


Fig. 5 Overflow potential ϕ_{of} and injection potential ϕ_{inj} vs the dose of B^+ -implantation.

The upper level of the dynamic range of photodiodes is limited by the saturation of electron storage in the n^+ -region and gives the saturated output voltage V_{so} from the built-in floating diffusion amplifier. The V_{so} values were measured as a function of V_{sub} at a constant reset voltage V_R of 8 V on two samples A and B with the p-wells formed by the B^+ implantation at doses of 5×10^{11} ions/cm² and 6×10^{11} ions/cm², respectively. The results are shown in Fig. 6. It is seen that the V_{so} value is constant in the V_{sub} range below a certain voltage depending on the B^+ implantation dose, above which the photodiode saturation level goes down. The fact implies that the critical value of V_{sub} provides the potential profile for excess electrons to start overflowing towards the N-substrate. It is to be noted that these V_{sub} values are in good agreement with those of the overflow potential ϕ_{of} in Fig. 5 which were independently obtained.

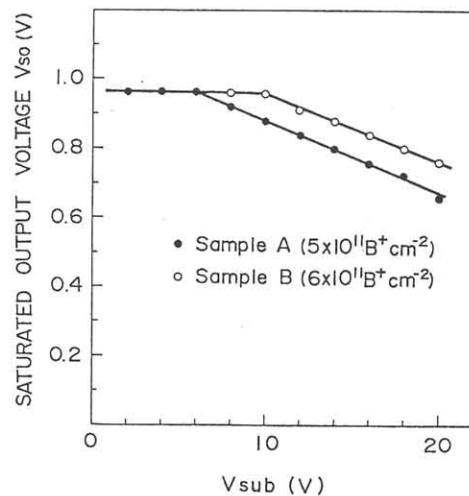


Fig. 6 The saturated output voltage V_{so} vs. supply voltage V_{sub} .

3.2 Blooming suppression

As described above, the infinite suppression of blooming in the p-well structure may be achieved if the voltage V_{sub} applied to the N-substrate is higher than the overflow potential V_{of} . However, at V_{sub} voltage slightly higher than ϕ_{of} , excess electrons due to over-exposure can not be fully drained to the substrate because of the slow drift velocity. There has been no established general rule for evaluation of the blooming suppression capability of the solid-state image sensors. In this paper, the blooming-suppression coefficient B_s is conveniently used, which is defined as the ratio of the maximum incident light intensity, above which the blooming-suppression becomes no longer capable, to the light intensity necessary for saturating the photodiodes. In Fig. 7, the blooming-suppression coefficients B_s measured with a light spot of a halogen lamp are plotted against the N-substrate voltage V_{sub} . As is seen in the figure, the higher V_{sub} is, the more effectively suppressed the blooming. On the other hand, the increase of V_{sub} narrows the dynamic range of photodiodes as discussed in section 3.1. In consideration of both the dynamic range of photodiode and the blooming suppression capability, V_{sub} in the sample A was chosen to be 12 V. As compared with the overflow drain structure in the conventional CPD image sensor, of which B_s is above 10, the new p-well structure has been found to be superior in the blooming suppression capability. An image reproduced with the sample A sensor is shown in Fig. 8.

The new CPD image sensor with the p-well structure has also achieved a high horizontal res-

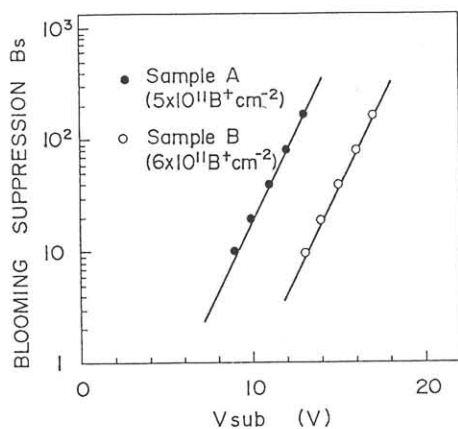


Fig. 7 The blooming-suppression coefficient B_s vs. supply voltage V_{sub} .

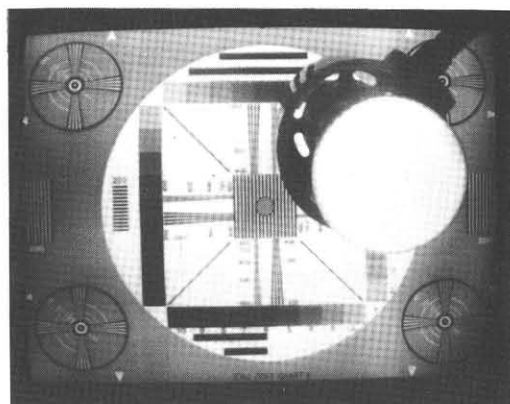


Fig. 8 An image reproduced by the new CPD image sensor with the p-well structure.

olution (480 TV lines). This has been realized by the checker pattern arrangement of photodiodes in the image area, from which the conventional overflow drain structure had been removed.

§4. Summary

A CPD image sensor with a p-well structure for blooming suppression has been proposed. The potential profile perpendicular to a photodiode in the p-well has been simulated by applying the linearly graded junction approximation to the numerical integration of the Poisson equation. Based on the simulation results, a CPD image sensor with the anti-blooming p-well structure has been designed and fabricated. It has been confirmed that the new structure is significantly effective in suppressing blooming. In addition, a high resolution has been obtained as a result of the application of the checker-pattern arrangement of photodiodes to the image area, from which the overflow drains had been removed.

Acknowledgement

The authors would like to express their gratitude to Dr. H. Mizuno and Dr. I. Teramoto for valuable discussion and encouragement. The support and assistance of many other research workers involved in this project are also acknowledged.

References

- 1) N. Koike et al : IEEE Trans. Electron Devices ED-27 (1980) 1676
- 2) Y. Ishihara et al : ISSCC Dig. Tech. Papers, Feb. (1980) 24
- 3) S. Terakawa et al : IEEE Electron Device Lett, EDL-1 (1980) 86